Lipopolysaccharide affects energy metabolism and elevates nicotinamide N-methyltransferase level in human aortic endothelial cells (HAEC)

Oksana Stępińska [a], Dorota Dymkowska [a,*], Łukasz Mateuszuk [b], Krzysztof Zabłocki [a,*]

[a] Laboratory of Cellular Metabolism, Nencki Institute of Experimental Biology, PAS, 3 Pasteura Str., 02–093 Warsaw, Poland
[b] Jagiellonian Centre for Experimental Therapeutics (JCET), Jagiellonian University, 14 Bobrzynskiego Str., 30–348 Krakow, Poland

ABSTRACT

This study aimed to investigate the putative role of nicotinamide N-methyltransferase in the metabolic response of human aortic endothelial cells. This enzyme catalyses S-adenosylmethionine-mediated methylation of nicotinamide to methylnicotinamide. This reaction is accompanied by the reduction of the intracellular nicotinamide and S-adenosylmethionine content. This may affect NAD^+ synthesis and various processes of methylation, including epigenetic modifications of chromatin. Particularly high activity of nicotinamide N-methyltransferase is detected in liver, many neoplasms as well as in various cells in stressful conditions. The elevated nicotinamide N-methyltransferase content was also found in endothelial cells treated with statins. Although the exogenous methylnicotinamide has been postulated to induce a vasodilatory response, the specific metabolic role of nicotinamide N-methyltransferase in vascular endothelium is still unclear. Treatment of endothelial cells with bacterial lipopolysaccharide evokes several metabolic and functional consequences which built a multifaceted physiological response of endothelium to bacterial infection. Among the spectrum of biochemical changes substantially elevated protein level of nicotinamide N-methyltransferase was particularly intriguing. Here it has been shown that silencing of the nicotinamide N-methyltransferase gene influences several changes which are observed in cells treated with lipopolysaccharide. They include altered energy metabolism and rearrangement of the mitochondrial network. A complete explanation of the mechanisms behind the protective consequences of the nicotinamide N-methyltransferase deficiency in cells treated with lipopolysaccharide needs further investigation.

1. Introduction

Bacterial lipopolysaccharide (LPS) is an endotoxin produced by gram-negative bacteria, which is neutralized under normal conditions by the innate immune system. This involves the activation of intracellular signalling pathways which are initiated by the activation of Toll-like receptor 4 (TLR4). LPS at high concentrations exerts toxic effects on cells, whereas at low concentrations promotes cell proliferation. In sepsis, the cellular response to LPS is strong and results in a generalized progressive inflammatory response (for rev. Fock and Parnova, 2021). Epidemiological studies indicate that LPS constitutes a risk factor for diseases such as atherosclerosis and diabetes (Chao et al., 2017). It was found that LPS not only activates endothelium indirectly through inflammatory mediators, such as tumour necrosis factor α (TNFα), interleukin-1β, interferons and others released from macrophages and immune cells (Gabarin et al., 2021; Meng and Lowell, 1997) but also directly due to stimulation of NO generation that supports vasodilatation (Chang et al., 2000). LPS increases endothelial permeability and leads to endothelial barrier dysfunction (Schlegel et al., 2009). Such impairments are behind cardiovascular diseases which are a leading health problem at least in developed countries, thus most studies on endothelium have been focused on searching for new therapies for these diseases. On the other hand, many aspects of cellular bioenergetics and the regulation of intermediary metabolic processes in endothelial cells are still unclear. It is generally accepted that the endothelial energy metabolism relies mostly on the glycolytic ADP phosphorylation while

the major mitochondrial role is to regulate intracellular calcium signalling and reactive oxygen species formation (Szewczyk et al., 2015). However, in pathological conditions, metabolic relations and the contribution of particular processes to global cellular metabolism are substantially changed (for rev see: Eelen et al., 2015).

Previously we showed that TNFα and palmitate affect mitochondrial network architecture and stimulate mitochondrial biogenesis. (Drabarek et al., 2012; Dymkowska et al., 2017). Furthermore, incubation of endothelial cells with statins results in cellular stress response accompanied by an elevation of nicotinamide-N-methyltransferase (NNMT) protein level (Dymkowska et al., 2021). This enzyme catalyses methyl group transfer from S-adenosylmethionine (SAM) to nicotinamide (NA). The reduction of NNMT gene expression was found to increase the detrimental effect of menadione. In turn, activation of NNMT/SIRT1 pathways seems to have a protective effect on increasing the survival rate of endothelial cells in oxidative stress conditions (Campagna et al. 2021a, 2021b). The product of the NNMT-catalysed reaction that is methylnicotinamide (MNA) modulates endothelial functions because of its anti-inflammatory and anti-thrombotic properties (Bartus et al., 2008; Chlopicki et al., 2007; Mateuszuk et al., 2020), stimulation of NO formation and modulation of lipid metabolism and storage, as well as lipoprotein and PGI2 levels (Nejabati et al., 2018). MNA may be also released to the extracellular venue (Mateuszuk et al., 2009).

Methylation of NA potentially reduces its availability for NAD^+ synthesis via the salvage pathway and therefore affects cellular redox processes and may limit sirtuin-catalysed deacetylation of many substrates including acetylated histones. An excessive NNMT activation also reduces SAM availability for other methylations. Both events may have epigenetic consequences. Thus NNMT forms a link between direct metabolic regulation and modification of gene expression (Roberti et al., 2021). NNMT is expressed in a variety of tissues and organs and an elevated amount of this cytosolic enzyme was found in many pathologies. Among them are Parkinson's disease (neurons), cirrhosis (liver), pulmonary disorders and a variety of different origin cancers (Roessler et al., 2005; Tomida et al., 2008; Sternak et al., 2010; Kim et al., 2010; Emanuelli et al., 2010, for rev see Roberti et al., 2021). It was also suggested that the elevated NNMT level could serve as a marker of some skin cancers although the role of this enzyme in carcinogenesis is not fully understood. This observation might be in line with the anti-cancerogenic properties of NA, however, it requires further investigation (Campagna et al., 2021b). Given all the aforementioned facts changes in cellular NNMT content and activity are common for diverse pathological conditions and have complex metabolic and physiological consequences. In previous experiments on endothelial energy metabolism, we used immortalised human endothelial cells EA.hy926. Here we have switched our interest to the primary human aortic endothelial cells and their metabolic response to bacterial lipopolysaccharide. We have focused our attention on the effects of LPS on mitochondria, intermediary energy metabolism and the putative role of NNMT in the cellular response to this lipopolysaccharide. We have found that LPS substantially increases NNMT protein level and silencing of the NNMT-encoding gene modifies some other cellular changes which emerged as a response to the LPS treatment. However, we have not confirmed a putative direct link between an elevated NNMT level and cellular NAD^+ content. Thus, in this study, we have pointed out the role of NNMT in the endothelial response to LPS while molecular mechanisms behind these effects remain obscure. A complete understanding of these processes needs further investigation.

2. Material and methods

2.1. Cell culture and treatment

HAECs were purchased from Lonza. Cells were grown in EGM BulletKit®−2 (Lonza) at 37°C in an atmosphere of 5% CO_2 and 95% air. The culture medium was composed exactly as recommended by the supplier (Lonza). Confluent cells were exposed to 100 ng/ml LPS (Escherichia coli O111:B4, List Biological Laboratories, #421) for a period within 0.5 h to 24 h as indicated in figure legends. In all experiments, cells of the third passage were used.

2.2. NNMT gene silencing

A freshly prepared mixture of NNMT-specific siRNA (ThermoFisher Scientific, #4390826) and jetPrime transfection reagent (PolyPlus transfection) was added to the confluent cells for 24 h. Then the silencing solution was replaced with a fresh culture medium and incubated for another 24 h before the treatment with LPS. The scrambled siRNA (ThermoFisher Scientific, #4390847) was used as a control. The efficiency of NNMT gene silencing was determined by Western Blot.

2.3. Cell lysis, and Western Blot analysis

Cell lysates were prepared as previously described (Drabarek et al., 2012). 30 μg of total protein was separated by polyacrylamide gel electrophoresis (PAGE) under denaturing conditions in the presence of 0.1% sodium dodecyl sulphate (SDS, BioShop) (Laemmli, 1970). After transferring to the PVDF membrane (Millipore) and blocking in 5% BSA for 1 h, proteins of interest were detected with specific primary antibodies (NNMT - 1:500, SantaCruz Biotechnology, sc-376048; ACC and p-ACC – 1:1000, Cell Signaling Technology, #3662 and #3676 respectively); anti-rabbit and anti-mouse secondary antibodies conjugated with horseradish peroxidase (HRP) were obtained from Abcam (1:5000 - ab6721, ab6728). For HRP detection (FusionFX, Vilber Lourmat) chemiluminescent substrate Immobilon Classico (Merck Millipore) was used. The optical density of bands corresponding to defined proteins was determined densitometrically with the BIO-1D software (Vilber Lourmat) and expressed in relation to β-actin (1:50000, Sigma, A-3854) used as a loading control.

2.4. Immunocytochemistry

Confluent cells grown on the collagen-coated coverslips (ɸ12 mm) were loaded with 100 nM MitoTracker Red CMXRos (Molecular Probes) as previously described (Dymkowska et al., 2021). After gentle rinsing, the cells were fixed with 4% paraformaldehyde, rinsed with PBS supplemented with 5% BSA, permeabilized with 0.1% Triton X-100 in 5% BSA and rinsed overnight with 1% BSA at 4°C. Finally, cells were stained with Actin-Stain 488 Phalloidin (1:1000; Cytoskeleton) and with 2 μg/ml Hoechst 33342 (ThermoFisher Scientific) Finally, cells were sealed in VECTASHIELD Mounting Medium (VECTOR Laboratories). Fluorescence microscopy analysis was carried out using a Zeiss Spinning Disc microscope.

2.5. Metabolite determination using the HPLC method

Cell monolayers were rinsed with cold 0.3 M mannitol and extracted with the mixture of methanol: acetonitrile: water (2:2:1). After centrifugation at 4 °C, supernatants were stored at − 80 °C and pellets were used for protein assay. Before metabolite measurement, each sample was supplemented with 140 pmoles of an appropriate standard. Metabolites were separated and quantitively analysed with the use of an ion-exchange chromatography system (Dionex ICS-3000 chromatograph, ThermoFisher Scientific) coupled with Waters ZQ mass spectrometer (Waters Corporation). Metabolite separation was performed on AS11-HC high-capacity anion-exchange column using 1–80 mM KOH gradient as the solvent. In the case of ATP, ADP and AMP measurements, an integrated Dionex chromatograph UV-detector (260 nm) was used. All samples were analysed quantitatively to the reference standard and cell protein.

To determine the extracellular methylnicotinamide level 100 μl aliquots of culture medium were frozen at − 80 °C. The cells were stored to
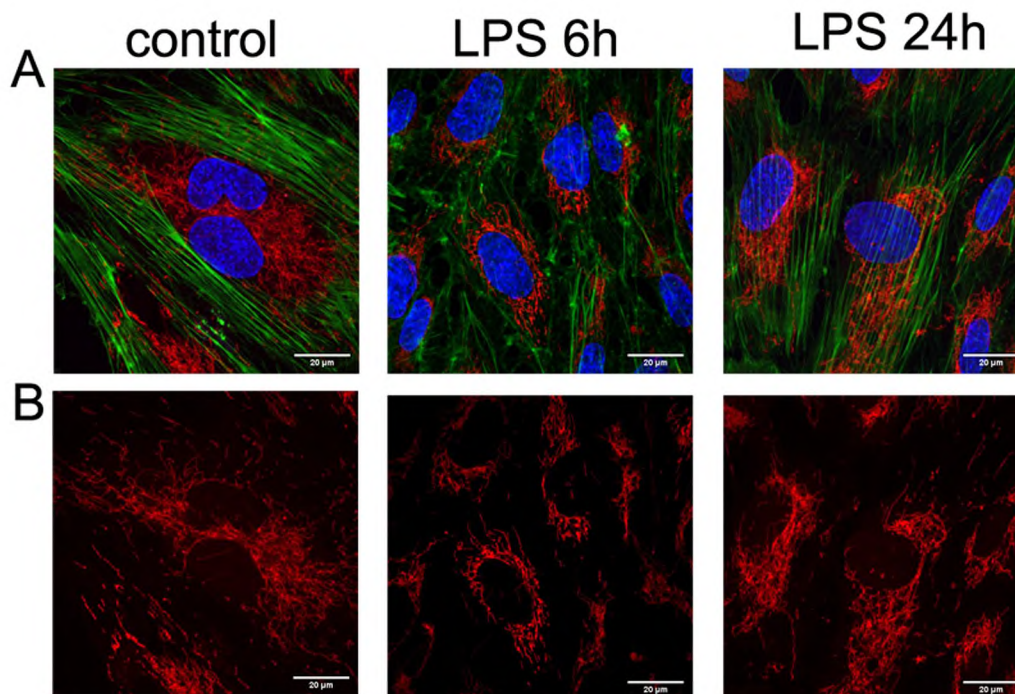
Fig. 1. Effect of LPS on mitochondrial network organization. **A.** Cytoskeleton and mitochondria in HAECs. **B.** Mitochondrial network organisation. Green – actin cytoskeleton stained with Actin-stain 488 phalloidin, Red – mitochondria labelled with MitoTracker CMXRos, Blue – nucleus with Hoechst 33342.

measure the total protein amount. Aliquots of 50 μl of medium were spiked with 5 μl of internal standard (deuterated analogues of the analyte) at the concentration of 25 μg/ml. Samples were subjected to deproteinization with 100 μl of acetonitrile acidified with 0.1% formic acid, vortexed, cooled at 4 °C for 15 min and centrifuged (15000xg, 15 min, 4 °C). Supernatants were injected into the LC column. Chromatographic analysis was performed using an UltiMate 3000 LC system (ThermoScientific Dionex) consisting of a pump (DGP-3600RS), a column compartment (TCC-3000RS), an autosampler (WPS-3000TRS), and an SRD-3600 solvent rack (degasser). Chromatographic separation was carried out on an Aquasil C18 analytical column (4.6 mm × 150 mm, 5 mm; ThermoScientific). MNA was eluted with the mobile phase consisting of acetonitrile and 5 mM ammonium formate in isocratic elution (80:20 v/v) at the flow rate of 0.8 ml/min. MNA detection was performed with the use of a TSQ Quantum Ultra mass spectrometer equipped with heated electrospray ionization (HESI-II) probe (ThermoScientific). The mass spectrometer was operating in the positive ionisation using selected reactions monitoring mode (SRM), monitoring the transition of the protonated molecular ions (for MNA Precursor $[m/z] = 137$, Product $[m/z] = 94$). Data acquisition and processing were accomplished using Xcalibur 2.1 software.

To measure cellular NAD^+ content the cells were rinsed with cold PBS and then extracted with an ice-cold 10% perchloric acid. Then the cells were harvested, transferred to Eppendorf tubes, forced through the thin needle, vortexed and incubated on ice for 15 min. Then, they were centrifuged at 15000xg at 4 °C for 5 min. The supernatants were transferred to fresh tubes, neutralized with 3 M potassium carbonate and centrifuged again at 15000xg at 4 °C for 5 min. Supernatants were transferred to fresh tubes and stored at − 80 °C. NAD^+ assays were made as described by Yoshino and Imai (2013).

2.6. Calcium measurement

Cytosolic Ca^{2+} concentration was measured with the fluorescent probe Fura-2-AM as described and calculated elsewhere (Onopiuk et al. 2015; Grynkiewicz et al., 1985) using a Hitachi F-7000 fluorimeter set.

2.7. Oxygen consumption

HAECs were grown in Seahorse XFe96 polystyrene tissue culture plates (Agilent) and stimulated with LPS upon reaching confluence. Before measurement, cells were incubated in Seahorse XF DMEM assay medium (without phenol red and Sodium Bicarbonate) containing 10 mM glucose, 1 mM pyruvate and 2 mM glutamine in a non-CO_2 incubator at 37 °C for 1 h. Oxygen consumption rate (OCR) was measured every 3 min with mixing of 3 min in each cycle, with 4 cycles per step using Seahorse XFe96 Analyzer (Agilent). Cell Mito Stress Test was used for assessing mitochondrial function. The sequential addition of oligomycin A (1.5 μM), FCCP (1.0 μM), and antimycin A/rotenone (0.5 μM) dissolved in DMEM assay medium allowed calculating of the OCR linked to ATP production, maximal respiration capacity and spare respiratory capacity. Basal respiration was measured before injection of oligomycin A.

2.8. Expression of the results

Analysis was performed using GraphPad Prism 9 software. The results are presented as means of ratios of treatment (experimental group) to control values ± SD for the number of separate experiments. Statistical significance of differences (p-values less than 0.05) was calculated using a one-way analysis of variance (ANOVA). Proper Multiple Range Tests were used for comparisons between experimental groups.

2.9. Protein assay

The total protein content was determined with a Bio-Rad protein assay according to the manufacturer's instructions.

3. Results

3.1. Response of control HAECs to LPS

In all experiments, LPS was used at a concentration of 100 ng/ml. It was the lowest one that was found to induce cellular response expressed
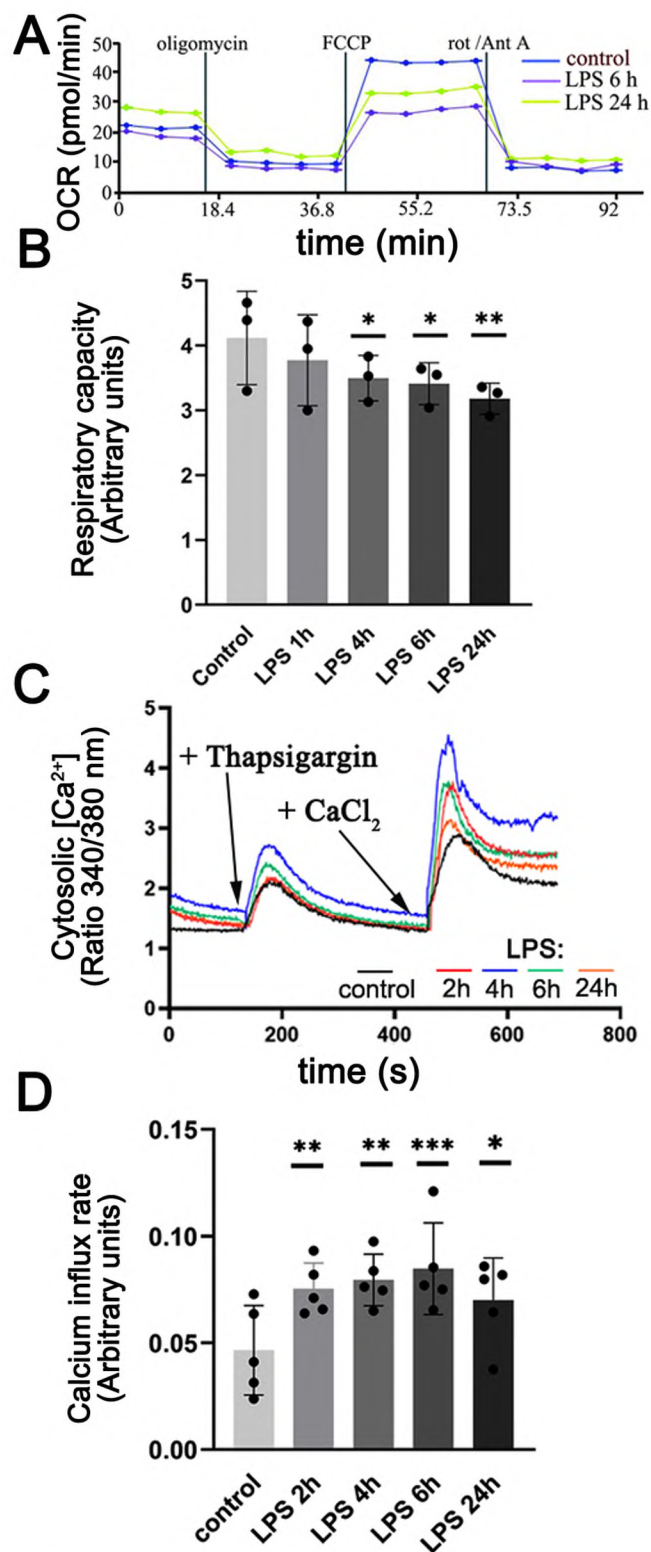
Fig. 2. Effect of LPS on oxygen consumption and store-operated calcium entry in HAECs. A and B oxygen consumption, C and D SOCE. Row data was obtained during direct oxygen consumption (representative experiment) and mitochondrial respiratory capacity (the ratio of maximal OCR after FCCP to minimal OCR after oligomycin) of control and LPS-treated cells. Slopes after the addition of CaCl$_2$ reflect rates of [Ca^{2+}]c elevation due to activated store-operated calcium entry, Data show mean values ± SD for n = 3–5, *p < 0.05, * *p < 0.005, * * *p < 0.002.
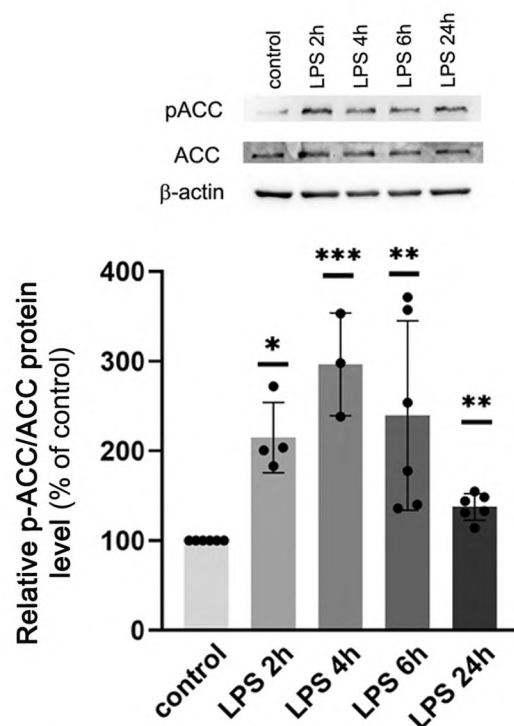

Fig. 3. Effect of LPS on acetyl-CoA kinase (ACC) phosphorylation in HAECs. The representative western blot and mean values ± SD for n = 3–6, *p < 0.05, * *p < 0.005, * * *p < 0.002.

as an elevation of the adhesion molecules ICAM-1 and VCAM-1 in HAECs (not shown).

Fluorescent microscopy indicates transient changes in the architecture of the mitochondrial network in HAECs treated with LPS (Fig. 1). Mitochondria evenly dispersed within control cells became more condensed in the perinuclear space in the 6th hour of LPS treatment and after the next 18 h, this effect substantially reverses.

LPS also strongly affects the oxidative phosphorylation in HAECs but this effect in contrast to the modified mitochondrial network organization does not reverse (Fig. 2). Fig. 2A shows representative traces obtained with the use of the Agilent Seahorse XFe96 analyser. Although at this stage of the experiment the traces are not normalized to the cellular protein they may be considered reliable as the cells were always seeded at the same density and the experiments were performed after the monolayer had reached complete confluency. Thus the number of cells in each well may be assumed as the same with a satisfying approximation. Fig. 2 B also points out changes in the respiratory chain capability, which represents the fraction of the respiratory chain activity attributed to covering the energy demands for ADP phosphorylation. These effects are accompanied by the deregulation of the store-operated calcium entry (SOCE) (Fig. 2C and 2D), and transiently increased ACC phosphorylation (Fig. 3). The latter indicates an elevation of the AMPK activity. LPS also induces substantial changes in the proportion of glycolytic and tricarboxylic acid cycle (TCA) intermediates (Fig. 4). Cross-over analysis indicates a transitory inhibition of pyruvate kinase followed by a complete recovery and reversed ratio between phosphoenolpyruvate and pyruvate (Fig. 4). Pyruvate accumulation may also be caused by an inhibition of the further steps of its oxidation by pyruvate dehydrogenase and then in the TCA cycle or the respiratory chain. An excess of pyruvate is converted to lactate by lactate dehydrogenase.

Effects of LPS on the adenine nucleotide content seem to be statistically insignificant though they exhibit the same tendency after 4, 6 and 24 h of the treatment. Thus some decrease in the ATP level could be considered to be potentially relevant. Finally, endothelial metabolism became more glycolytic but still efficient to deliver an ample amount of
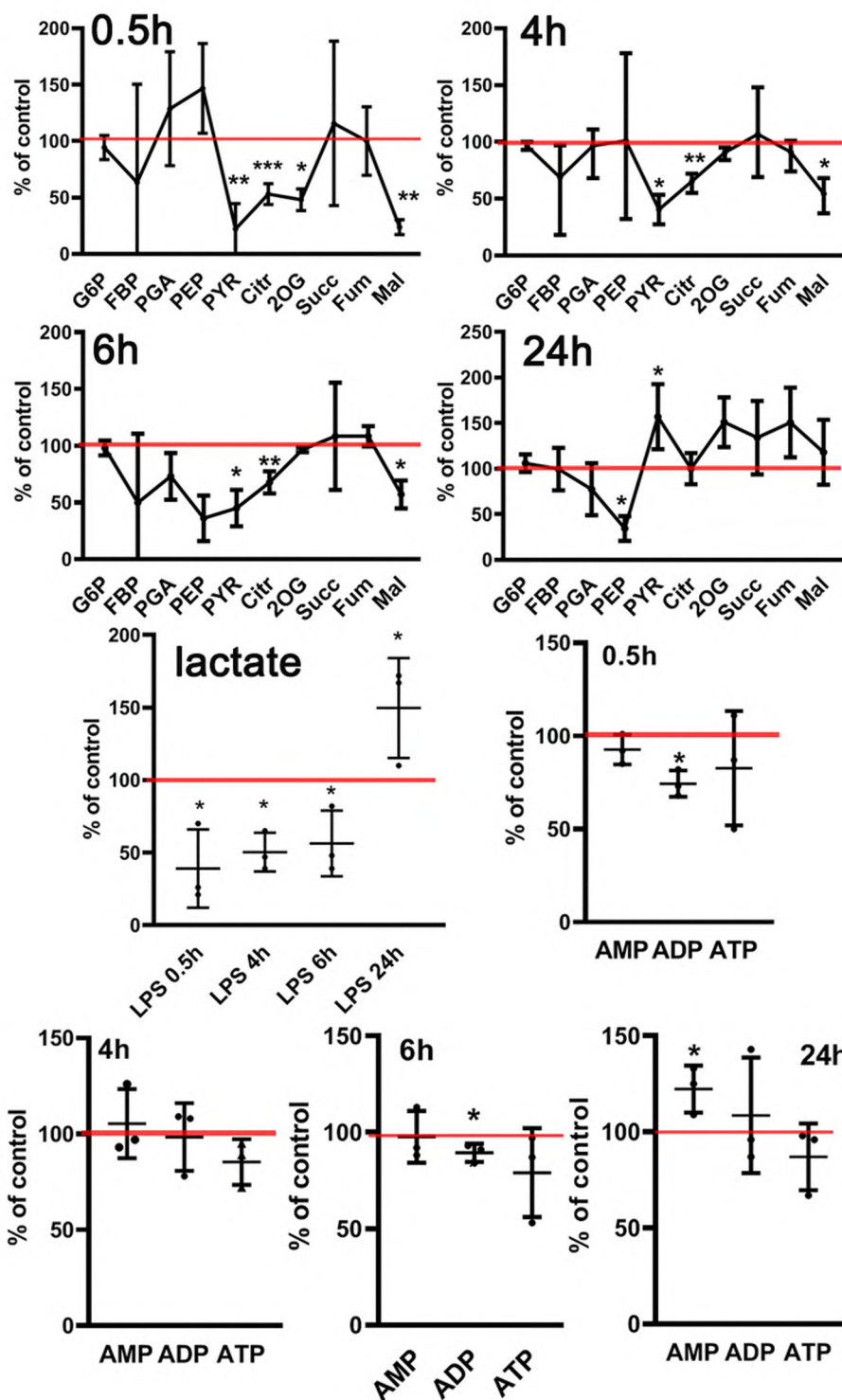
Fig. 4. Effect of LPS on the relative metabolite and adenine nucleotide content. Cross-over graphs show mean values $\pm$ SD of the relative change of tested parameter vs. untreated control cells assumed as 100% (red line). n = 3, *P < 0.05, * *p < 0.005, * * *p < 0.0005.

ATP.

Our previously published data (Dymkowska et al., 2021) and results published by other authors (Akar et al., 2020) indicate that treatment of cells with various stimuli results in an elevation of NNMT content. This effect could imply changes in the cellular energy metabolism (Mistry et al., 2020). Similarly, as is shown in Fig. 5 LPS induces an elevation of NNMT level in HAECs. Despite these changes, the amount of MNA released from cells treated with LPS to the extracellular milieu is much lower than that in the case of untreated HAECs (Fig. 7B, compare the first bars from each set of three). It shows that the LPS-induced increase in the amount of NNMT detected by the Western Blot does not correspond with NNMT activity at least estimated on a basis of extracellular MNA level. Moreover, the substantial descendant effect on MNA level is not accompanied by changes in the NAD^+ content (Fig. 7C, compare the first bars from each set of three). To test whether the LPS-induced increase in the NNMT level is of any importance for the cellular metabolic response to this lipopolysaccharide, HAECs with silenced NNMT-encoding gene were used.
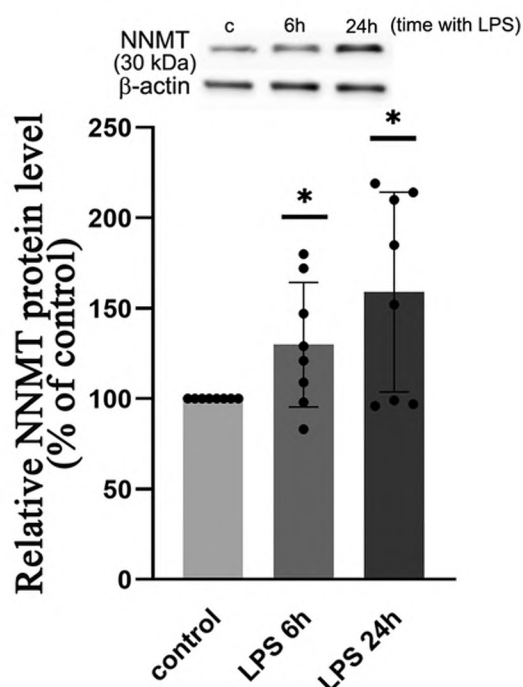
Fig. 5. LPS increases NNMT level after 6 and 24 h of incubation. Bars show relative data from 7 independent experiments. NNMT protein level was assumed to be 100%. Data shown as mean ± SD, n = 7, * p < 0.05. Above the bars, a Western Blot from one experiment is shown.

3.2. Response of HAECs with silenced NNMT gene to LPS

The incubation of HAECs with NNMT-siRNA substantially reduces the NNMT protein level (Fig. 6A). This effect is accompanied by a substantial reduction of MNA (Fig. 6B) while the NAD^+ content remains unaffected (Fig. 6C). The reduction of the NNMT level persists for at least 48, i.e. 24 h after the addition of siRNA plus 24 h in the presence of LPS but without any additional supplementation with siRNA (Fig. 7A, dark bars).

Preincubation of cells with scrambled siRNA does not diminish the stimulatory effect of LPS on the NNMT level (Fig. 7A, bright bars).

Fig. 7B confirms the data shown in Fig. 6B and shows that silencing of the NNMT gene reduces the amount of extracellular MNA (the first set of three bars). LPS reversibly reduces MNA formation in the control cells while in the cells with silenced NNMT gene this inhibitory effect is much deeper and persists at least for 24 h. Finally, cellular NAD^+ content remains unchanged regardless of the mechanisms behind the reduced MNA formation (Fig. 7C). Silencing of the NNMT gene seems to gently (insignificantly in terms of statistics) prevent LPS-evoked stimulation of SOCE (Fig. 7D).

Moreover, the LPS-induced changes in the mitochondrial network architecture in HAECs are less visible in the cells with silenced NNMT gene than in their equivalents treated with scrambled RNA (Fig. 8) or in the case of the control cells (see Fig. 1). Silencing of NNMT-gene also weakened the LPS-evoked effect on the relative metabolite content in HAECs (Fig. 9). As shown in Fig. 9 column B, LPS substantially reduces the level of most of the metabolites involved in glycolysis and the Krebs cycle in cells with unaffected NNMT gene expression (scrambled RNA) while this effect is less profound in cells with silenced NNMT (Fig. 9C). More comprehensive data concerning these experiments are shown in Suppl. 1 where A and B correspond to data shown in Fig. 9B and C while Suppl. 1C clearly shows that silencing of the NNMT encoding gene diminishes or reverses the effects of LPS visualised in Fig. 9B and Suppl. 1A. This is visible despite some differences between cells exposed to LPS alone and those exposed to LPS but pre-treated with the scrambled
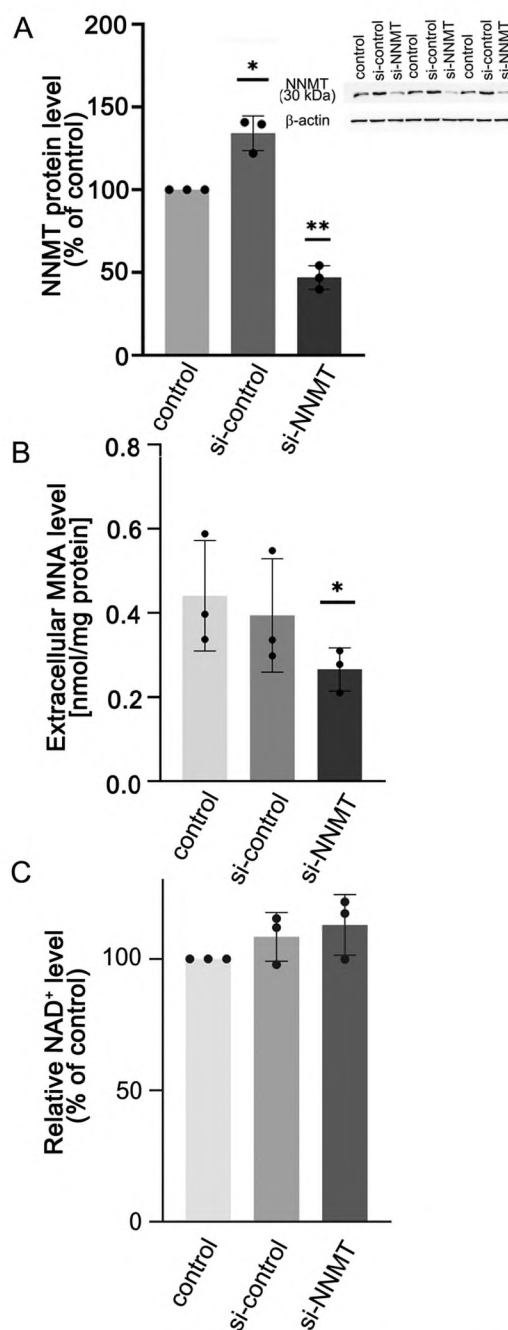

Fig. 6. Effect of silencing of the NNMT-encoding gene on NNMT protein level (A), MNA generation (B) and NAD^+ content (C) 48 h after addition of siRNA to the confluent cells. NNMT level was estimated with Western Blot. The representative result is shown above the graph. Data shown as mean±SD, n = 3–8; *p < 0.05, * *p < 0.005.

siRNA (compare Fig. 4A and Fig. 9B). The effect of the transfection procedure itself (si-NNMT RNA vs. scrambled RNA) on the metabolite profile is shown in Fig. 9A and reproduced in Suppl. 1D.

4. Discussion

Effects of LPS on endothelial physiology, inflammatory response and NO generation have been broadly discussed for a long time (Chao et al., 2017; Dauphinee and Karsan, 2006; Dayang et al., 2019; Li et al., 2017; You et al., 2021). However, a detailed understanding of biochemical processes particularly focused on the energy metabolism in human endothelium upon treatment with LPS needs further study. This issue
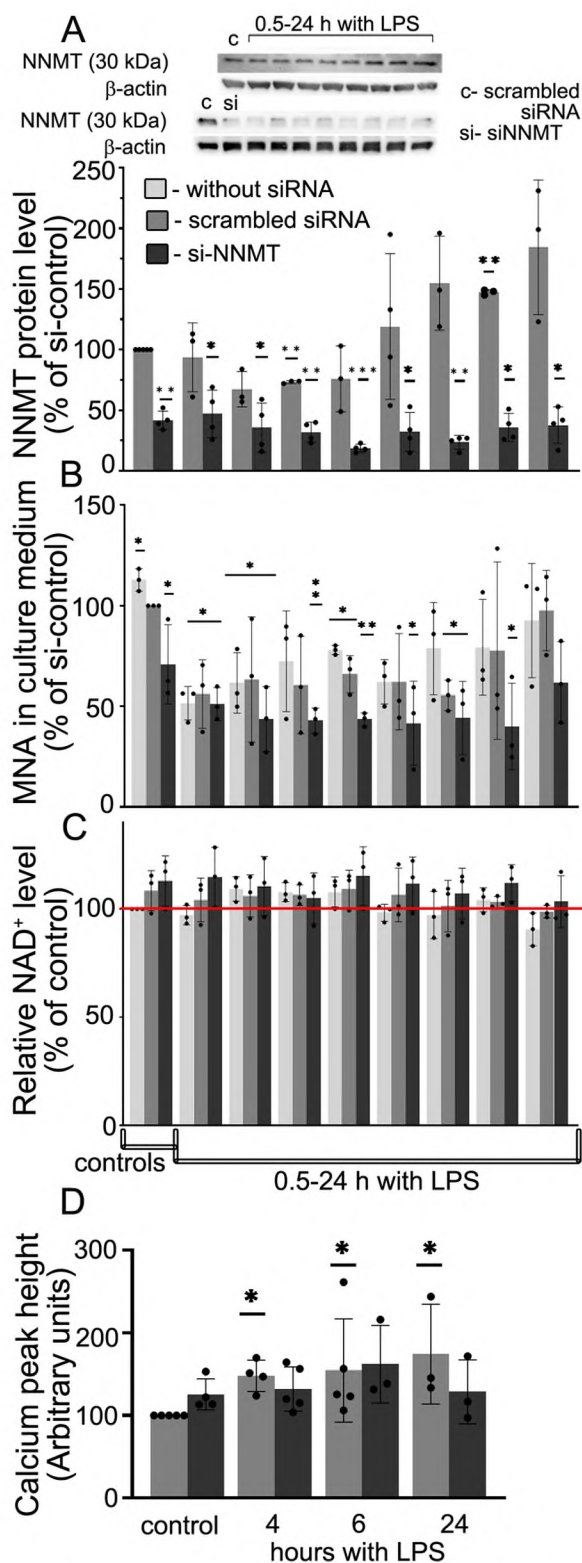
Fig. 7. Effect of LPS on NNMT (A), MNA (B), NAD$^+$ level (C) and thapsigargin-induced calcium response (SOCE; D) in HAECs with silenced NNMT gene. Each bar indicates mean values ± SD of the relative change of tested parameter vs. untreated control cells (no silencing, no LPS) assumed as 100%, n = 3–8, *p < 0.05; * *p < 0.005, * * *p < 0.0005. A representative NNMT Western Blot is shown above graph A.

seems to be particularly interesting because LPS substantially affects endothelial signal transduction which is behind the physiological responses of the endothelium to a variety of stimuli. Calcium signalling and energy metabolism are mutually dependent factors that are of high importance for all cell types, but endothelium has been poorly characterized in this matter. LPS was found to induce FADD-mediated endothelial cell apoptosis (Choi et al., 1998) thus many studies focused on the harmful effects of lipopolysaccharide and the reduced viability of endothelial cells (Chen and Song, 2020). Though LPS-induced and TLR4-mediated signalling in endothelial cells has been broadly investigated (Dauphinee and Karsan, 2006), experimental efforts were primarily focused on searching for potential therapeutic approaches to prevent sepsis and serious cardiovascular complications.

In the present study, we have investigated the effects of the relatively gentle treatment of cells with LPS to follow adaptive response without affecting cell viability. Thus, to minimize potential side effects of LPS, in all experiments presented here, it was used at the lowest concentration and applied for the period which was established experimentally to be sufficient to elevate the protein level of the adhesive molecules but not reduce cell survival.

4.1. LPS affects endothelial bioenergetics

Mitochondria in the endothelial cells are not in the centre of ATP generation but their role as a hub of the cellular calcium signalling in all mammalian cells is unquestionable (Szewczyk et al., 2015). Substantially but reversibly changing the architecture of the mitochondrial network indicates mitochondrial involvement in the response of HAECs to LPS. Similar effects we have previously observed in EA.hy926 cells stimulated with TNFα (Drabarek et al., 2012; Dymkowska et al., 2019]. The LPS effect on changes in the metabolite profile indicates a reversible inhibition of pyruvate kinase, which is the regulatory enzyme that catalyses PEP utilization for pyruvate formation. While the first phase of the changes (increased PEP level) does not have a clear explanation at the moment, the progressive accumulation of pyruvate is in line with LPS-induced elevation of PKM2 (pyruvate kinase isoform M2) activity that was observed in macrophages exposed to the lipopolysaccharide for 24 h (Palsson-McDermott et al., 2015). These effects are accompanied by substantially elevated levels of Krebs cycle intermediates probably potentiated due to inhibited mitochondrial NADH reoxidation through the respiratory chain. The increased level of lactate confirms a rise in anaerobic processes which allow cells to restore the pool of NAD$^+$. Both the reduced oxidative metabolism and stimulation of glycolysis were previously described for various experimental models of inflammation (Robb et al., 2020; Vijayan et al., 2019; Yarbro and Pence, 2019). The relatively stable or only slightly reduced level of ATP indicates that the cellular bioenergetics, despite its shift towards a more glycolytic mode, remains sufficient. On the other hand, some elevation in the AMP content might suggest activation of AMPK. The latter assumption is additionally strengthened as the proportion of phosphorylated form of ACC is increased in LPS-treated HAECs. A putative mechanism that is behind reduced oxidative phosphorylation seems not to be clear (Kelly and O'Neill, 2015). Moderately increased cytosolic Ca^{2+} concentration should accelerate mitochondrial energy processes by stimulation of the TCA cycle. However, inhibition of the respiratory chain may have a superior effect and secondarily inhibits downstream metabolic processes delivering reduced nucleotides (NADH and FADH$_2$), such as the TCA cycle.

It is possible that changes in the cellular calcium response are secondary and attributed to the reorganized mitochondrial network architecture and affected mitochondrial Ca^{2+}-buffering capacity. The transient increase in ACC phosphorylation shown in Fig. 3 reflects an elevated AMPK activity and corresponds with the time course of changes in cellular lactate content. Interestingly, elevated activity of AMPK was implicated as one of the factors in a down-regulation of glycolysis in vascular endothelial cells subjected to pulsatile shear stress (Han et al.,
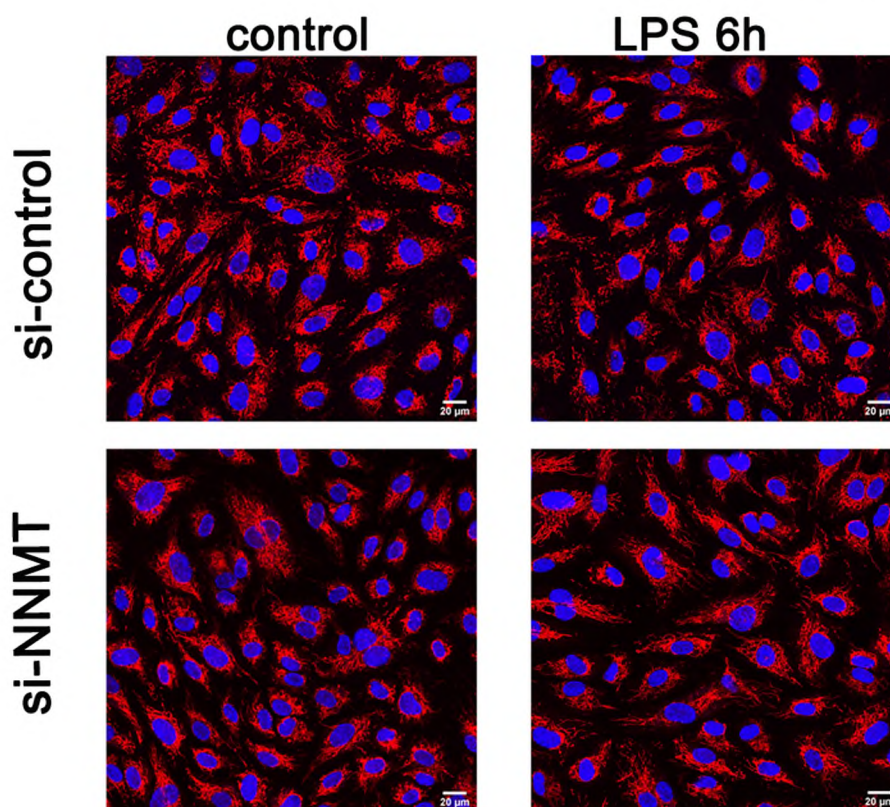
Fig. 8. Effect of LPS on the mitochondrial network in HAECs with silenced NNMT-encoding gene. Red – mitochondria labelled with Mitotracker CMXRos, Blue – nucleus with Hoechst 33342.

2021). However, in our static experiments (without any medium flow), shear stress cannot be considered. AMPK was found to indirectly induce PDK4 gene expression thereby inhibiting pyruvate dehydrogenase activity (Fritzen et al., 2015). AMPK also activates PDHc through phosphorylating catalytic subunit PDHA which alleviates inhibitory phosphorylation catalysed by PDKa. It stimulates the TCA cycle as was observed in the metastatic cancer cells (Cai et al., 2020]. It seems that AMPK interacts with several, sometimes counteracting processes so the resultant, tissue-specific effect reflects a precisely regulated and changing metabolic balance.

The cellular concentration of the crucial metabolic intermediates has a key role in metabolic regulation and coordination of multiple metabolic processes. One of such factors is NAD^+, a broadly used electron and proton acceptor in many intracellular redox reactions. Its reduced form (NADH) is oxidized in the respiratory chain which is a major energy transducing process in almost all animal cells. Moreover, NAD^+ is used as a cofactor for sirtuins which are metabolic regulators in mammals (Begum et al., 2021). Therefore, the cellular concentration of NAD^+ must be controlled and maintained at an appropriate level. This in turn implies that excessive consumption of NAD^+ precursors by alternative processes may be a limiting factor for NAD^+ formation. Recently great attention has been focused on nicotinamide methylation catalysed by NNMT. This reaction competes for nicotinamide with nicotinamide phosphoribosyltransferase and potentially may limit NAD^+ synthesis. Moreover, nicotinamide methylation needs a methyl group donor that is S-adenosyl methionine. Therefore, an elevated NNMT activity may also affect other SAM-mediated methylation reactions. A growing body of evidence indicates that NNMT has a crucial regulatory function influencing not only energy metabolism but also epigenetic regulation in a variety of tissues (Sperber et al., 2015; Ulanovskaya et al., 2013; and for rev. Roberti et al., 2021). However, the physiological role of this enzyme in vascular endothelial cells is still obscure. Experimental data concerning NNMT clearly show that EA.hy926 cells challenged by statins

exhibit an elevated level of this protein, which may reflect cellular stress response (Dymkowska et al., 2021). Moreover, NNMT activation may contribute to the pathological processes; an elevated content of this enzyme was found in a course of some pathologies including hepatocellular carcinoma, breast cancer and stroma of colorectal cancer (Eckert et al., 2019; Li et al., 2019; Yang et al., 2021; Wang et al., 2019).

Here we have observed a time-dependent elevation of the NNMT protein level in cells treated with LPS but we have not confirmed an expected elevation of the MNA level (see Fig. 6B, the first bars in each time point). In contrast, it was substantially reduced as soon as 30 min after the addition of LPS to the growth medium and though gradually increased together with increasing NNMT level, it never reached the control value as in cells untreated with LPS. It suggests additional effects of lipopolysaccharide attenuating an activity of NNMT-catalysed reaction. It also explains why we have not found any differences in the NAD^+ level in comparison to the control cells regardless of the time of treatment with LPS (Fig. 7C). It is also possible that NAD^+ synthesis in HAECs occurs through alternative pathways, thus changes in nicotinamide level have not any impact on this process (Covarrubias et al., 2021; Liu et al., 2018).

4.2. Silencing of NNMT-encoding gene prevents LPS-evoked effects

The direct link between LPS-evoked elevation of NNMT content and changes in the mitochondrial organization seems to be ambiguous. LPS only transiently affects the mitochondrial network architecture which coincides with substantial and progressive changes in the NNMT level (see Figs. 1 and 5). On the other hand, silencing of the NNMT encoding gene protects the mitochondrial network from LPS-induced reorganization (see Fig. 8). This might suggest that the LPS-evoked effect on the NNMT level is a more or less direct cause of changes in the mitochondrial network architecture as it must precede or co-exist with them. The reduction of the NNMT level before the treatment with LPS prevents its
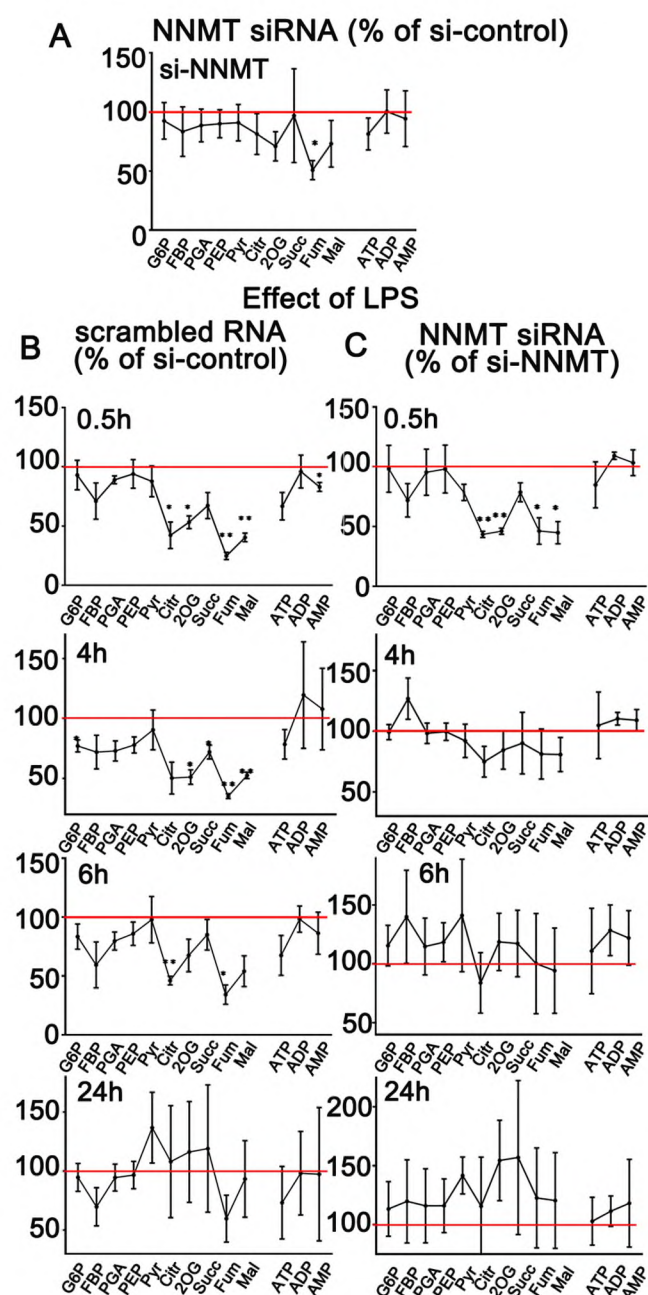
Fig. 9. Effect of LPS and NNMT gene silencing on glycolytic and Krebs cycle metabolite content in HAECs. A: Effect of NNMT gene silencing with siRNA vs. the effect of treatment of cells with scrambled RNA; **Column B:** Effect of LPS on cells treated with scrambled RNA vs. without LPS; **Column C:** Effect of LPS on cells treated with siRNA (silenced NNMT gene) vs. without LPS. The red line in each graph represents appropriate control without LPS, n = 3, *p < 0.05, * *p < 0.005.

detrimental effect. Presented data do not allow identifying a mechanism behind the counteracting effect of NNMT gene silencing on the LPS-induced metabolic effects. Interestingly silencing of the NNMT gene itself does not influence the level of metabolites but fumarate whose concentration was substantially reduced. It might result from increased methylation of SDH gene promoter and reduced SDH transcription rate (Aggarwal et al., 2021, and for rev. Hawkins et al., 2018].

Results presented hitherto are not sufficient to coherently explain the link between LPS-induced effects in HAECs and NNMT activity. The elevation of the NNMT level in the response to the LPS treatment doesn't seem to be adaptive in the sense of "protecting" as the silencing of the

NNMT gene abolishes some effects of LPS. Faster restoration of the TCA metabolite profile (Fig. 9 and Suppl. 1) in the LPS-treated cells with the reduced NNMT level is a good exemplification supporting such an assessment. One could speculate that the aberrant Ca^{2+} homeostasis may be involved in the LPS/NNMT interplay but it needs additional experimental confirmation. Recently a mechanism behind the activation of SOCE in HUVECs treated with LPS has been precisely described (Qiu et al., 2021). The experiments shown here indicate substantially increased calcium response of HAECs exposed to LPS upon SOCE activation with thapsigargin. Silencing of the NNMT-encoding gene slightly counteracts such a response, which makes the role of Ca^{2+} signalling in this context potentially relevant. We suppose that the restoration of calcium signalling may be at the bottom of the remaining effects of NNMT elimination but it requires deeper study to be confirmed. Furthermore, we did not investigate the putative effects of LPS on methylation processes. This issue needs more precisely addressed investigation.

5. Conclusions

It seems to be clear that silencing of the NNMT encoding gene and therefore reduction of the NNMT protein content and activity influences HAECs in a metabolic point(s) located "above" several important regulatory phenomena such as calcium response and rearrangement of mitochondrial network architecture. Thus, the regulation of NNMT activity is of paramount importance for crucial metabolic processes in endothelial cells, which outreaches earlier described the vasculo-protective role of this enzyme presumably by delivering MNA (Fedor-owicz et al., 2016; Przyborowski et al., 2015). We assume that the metabolic consequences of NNMT shown here unveil the tip of the iceberg. Because NNMT stands at the crossroads of metabolic pathways and epigenetic regulatory processes the complete understanding of its role not only in the endothelial cells but also in many others seems to be very difficult and requires multilateral approaches. It is tempting to speculate that NNMT could be considered a potential therapeutic target and this aspect was also pointed out by others (Gao et al., 2021).

CRediT authorship contribution statement

Oksana Stępinska: Experimentation, Dorota Dymkowska: Experimentation and original draft preparation, Łukasz Mateuszuk: Experimentation (HPLC), Krzysztof Zabłocki: Conceptualization, Supervision, Writing.

Declaration of Interest Statement

none.

Appendix A. Supporting information

Supplementary data associated with this article can be found in the online version at doi:10.1016/j.biocel.2022.106292.

References

Aggarwal, R.K., Luchtel, R.A., Machha, V., Tischer, A., Zou, Y., Pradhan, K., Ashai, N., Ramachandra, N., Albanese, J.M., Yang, J.I., Wang, X., Aluri, S., Gordon, S., Aboumohamed, A., Gartrell, B.A., Hafizi, S., Pullman, J., Shenoy, N., 2021. Functional succinate dehydrogenase deficiency is a common adverse feature of clear cell renal cancer. e2106947118 Proc. Natl. Acad. Sci. USA 118 (39). https://doi.org/10.1073/pnas.2106947118.

Akar, S., Harmankaya, İ., Uğraş, S., Çelik, Ç., 2020. Expression and Clinical Significance of Nicotinamide N-Methyltransferase in Cervical Squamous Cell Carcinoma. Int. J. Gynecol. Pathol. 39 (3), 289–295. https://doi.org/10.1097/PGP.0000000000000605.

Bartus, M., Łomnicka, M., Kostogrys, R.B., Kaźmierczak, P., Watała, C., Słominska, E.M., Smoleński, R.T., Pisulewski, P.M., Adamus, J., Gebicki, J., Chlopicki, S., 2008. 1-Methylnicotinamide (MNA) prevents endothelial dysfunction in hypertriglyceridemic and diabetic rats. Pharmacol. Rep. 60 (1), 127–138.

Begum, M.K., Konja, D., Singhn, S., Chlopicki, S., Wang, Y., 2021. Endothelial SIRT1 as a Target for the Prevention of Arterial Aging: Promises and Challenges. J. Cardiovasc. Pharmacol. 78 (Suppl 6), S63–S77. https://doi.org/10.1097/FJC.0000000000001154.

Cai, Z., Li, C.F., Han, F., Liu, C., Zhang, A., Hsu, C.C., Peng, D., Zhang, X., Jin, G., Rezaeian, A.H., Wang, G., Zhang, W., Pan, B.S., Wang, C.Y., Wang, Y.H., Wu, S.Y., Yang, S.C., Hsu, F.C., D'Agostino Jr, R.B., Furdui, C.M., Kucera, G.L., Parks, J.S., Chilton, F.H., Huang, C.Y., Tsai, F.J., Pasche, B., Watabe, K., Lin, H.K., 2020. Phosphorylation of PDHA by AMPK Drives TCA Cycle to Promote Cancer Metastasis. e7 Mol. Cell. 80 (2), 263–278. https://doi.org/10.1016/j.molcel.2020.09.018.

Campagna, R., Mateuszuk, Ł., Wojnar-Lason, K., Kaczara, P., Tworzydło, A., Kij, A., Bujok, R., Mlynarski, J., Wang, Y., Sartini, D., Emanuelli, M., Chlopicki, S., 2021. Nicotinamide N-methyltransferase in endothelium protects against oxidant stress-induced endothelial injury. Biochim. Biophys. Acta Mol. Cell. Res. 1868 (10), 119082 https://doi.org/10.1016/j.bbamcr.2021.119082.

Campagna, R., Pozzi, V., Sartini, D., Salvolini, E., Brisigotti, V., Molinelli, E., Campanati, A., Offidani, A., Emanuelli, M., 2021a. Beyond Nicotinamide Metabolism: Potential Role of Nicotinamide *N*-Methyltransferase as a Biomarker in Skin Cancers. Cancers 13, 4943. https://doi.org/10.3390/cancers13194943.

Chang, C.Y., Tucci, M., Baker, R.C., 2000. Lipopolysaccharide-stimulated nitric oxide production and inhibition of cell proliferation is antagonized by ethanol in a clonal macrophage cell line. Alcohol 20 (1), 37–43. https://doi.org/10.1016/s0741-8329(99)00054-3.

Chao, H.H., Chen, P.Y., Hao, W.R., Chiang, W.P., Cheng, T.H., Loh, S.H., Leung, Y.M., Liu, J.C., Chen, J.J., Sung, L.C., 2017. Lipopolysaccharide pretreatment increases protease-activated receptor-2 expression and monocyte chemoattractant protein-1 secretion in vascular endothelial cells. J. Biomed. Sci. 24 (1), 85. https://doi.org/10.1186/s12929-017-0393-1.

Chen, X., Song, D., 2020. LPS promotes the progression of sepsis by activation of lncRNA HULC/miR-204-5p/TRPM7 network in HUVECs. BSR20200740 Biosci. Rep. 40 (6). https://doi.org/10.1042/BSR20200740.

Chlopicki, S., Swies, J., Mogielnicki, A., Buczko, W., Bartus, M., Lomnicka, M., Adamus, J., Gebicki, J., 2007. 1-Methylnicotinamide (MNA), a primary metabolite of nicotinamide, exerts anti-thrombotic activity mediated by a cyclooxygenase-2/prostacyclin pathway. Br. J. Pharm. 152 (2), 230–239. https://doi.org/10.1038/sj.bjp.0707383.

Choi, K.B., Wong, F., Harlan, J.M., Chaudhary, P.M., Hood, L., Karsan, A., 1998. Lipopolysaccharide mediates endothelial apoptosis by a FADD-dependent pathway. 20185-10188 J. Biol. Chem. 273 (32). https://doi.org/10.1074/jbc.273.32.20185.

Covarrubias, A.J., Perrone, R., Grozio, A., Verdin, E., 2021. NAD+ metabolism and its roles in cellular processes during ageing. Nat. Rev. Mol. Cell. Biol. 22 (2), 119–141. https://doi.org/10.1038/s41580-020-00313-x.

Dauphinee, S.M., Karsan, A., 2006. Lipopolysaccharide signaling in endothelial cells. Lab. Invest 86 (1), 9–22. https://doi.org/10.1038/labinvest.3700366.

Dayang, E.Z., Plantinga, J., Ter Ellen, B., van Meurs, M., Molema, G., Moser, J., 2019. Identification of LPS-Activated Endothelial Subpopulations With Distinct Inflammatory Phenotypes and Regulatory Signaling Mechanisms. Front. Immunol. 10, 1169. https://doi.org/10.3389/fimmu.2019.01169.

Drabarek, B., Dymkowska, D., Szczepanowska, J., Zabłocki, K., 2012. TNFα affects energy metabolism and stimulates biogenesis of mitochondria in EA.hy926 endothelial cells. Int. J. Biochem. Cell. Biol. 44 (9), 1390–1397. https://doi.org/10.1016/j.biocel.2012.05.022.

Dymkowska, D., Kawalec, M., Wyszomirski, T., Zabłocki, K., 2017. Mild palmitate treatment increases mitochondrial mass but does not affect EA.hy926 endothelial cells viability. Arch. Biochem. Biophys. 634, 88–95. https://doi.org/10.1016/j.abb.2017.10.006.

Dymkowska, D., Drabarek, B., Michalik, A., Nowak, N., Zabłocki, K., 2019. TNFα stimulates NO release in EA.hy926 cells by activating the CaMKKβ-AMPK-eNOS pathway. Int. J. Biochem. Cell. Biol. 106, 57–67. https://doi.org/10.1016/j.biocel.2018.11.010.

Dymkowska, D., Wrzosek, A., Zabłocki, K., 2021. Atorvastatin and pravastatin stimulate nitric oxide and reactive oxygen species generation, affect mitochondrial network architecture and elevate nicotinamide N-methyltransferase level in endothelial cells. J. Appl. Toxicol. 41 (7), 1076–1088. https://doi.org/10.1002/jat.4094.

Eckert, M.A., Coscia, F., Chryplewicz, A., Chang, J.W., Hernandez, K.M., Pan, S., Tienda, S.M., Nahotko, D.A., Li, G., Blaženović, I., Lastra, R.R., Curtis, M., Yamada, S.D., Perets, R., McGregor, S.M., Andrade, J., Fiehn, O., Moellering, R.E., Mann, M., Lengyel, E., 2019. Proteomics reveals NNMT as a master metabolic regulator of cancer-associated fibroblasts. Nature 569 (7758), 723–728. https://doi.org/10.1038/s41586-019-1173-8.

Eelen, G., de Zeeuw, P., Simons, M., Carmeliet, P., 2015. Endothelial cell metabolism in normal and diseased vasculature. Circ. Res 116 (7), 1231–1244. https://doi.org/10.1161/CIRCRESAHA.116.302855.

Emanuelli, M., Santarelli, A., Sartini, D., Ciavarella, D., Rossi, V., Pozzi, V., Rubini, C., Lo Muzio, L., 2010. Nicotinamide N-Methyltransferase upregulation correlates with tumour differentiation in oral squamous cell carcinoma. Histol. Histopathol. 25 (1), 15–20. https://doi.org/10.14670/HH-25.15.

Fedorowicz, A., Mateuszuk, Ł., Kopec, G., Skórka, T., Kutryb-Zając, B., Zakrzewska, A., Walczak, M., Jakubowski, A., Łomnicka, M., Słomińska, E., Chlopicki, S., 2016. Activation of the nicotinamide N-methyltransferase (NNMT)-1-methylnicotinamide (MNA) pathway in pulmonary hypertension. Respir. Res. 17 (1), 108. https://doi.org/10.1186/s12931-016-0423-7.

Fock, E.M., Parnova, R.G., 2021. Protective Effect of Mitochondria-Targeted Antioxidants against Inflammatory Response to Lipopolysaccharide Challenge: A Review. Pharmaceutics 13 (2), 144. https://doi.org/10.3390/pharmaceutics13020144.

Fritzen, A.M., Lundsgaard, A.M., Jeppesen, J., Christiansen, M.L., Biensø, R., Dyck, J.R., Pilegaard, H., Kiens, B., 2015. 5'-AMP activated protein kinase α2 controls substrate metabolism during post-exercise recovery via regulation of pyruvate dehydrogenase kinase 4. J. Physiol. 593 (21), 4765–4780. https://doi.org/10.1113/JP270821.

Gabarin, R.S., Li, M., Zimmel, P.A., Marshall, J.C., Li, Y., Zhang, H., 2021. Intracellular and Extracellular Lipopolysaccharide Signaling in Sepsis: Avenues for Novel Therapeutic Strategies. J. Innate. Immun. 13 (6), 323–332. https://doi.org/10.1159/000515740.

Gao, Y., Martin, N.I., van Haren, M.J., 2021. Nicotinamide N-methyl transferase (NNMT): An emerging therapeutic target. Drug Discov. Today 26 (11), 2699–2706. https://doi.org/10.1016/j.drudis.2021.05.011.

Grynkiewcz, G., Poenie, M., Tsien, R.Y., 1985. A new generation of Ca2+ indicators with greatly improved fluorescence properties. J. Biol. Chem. 260 (6), 3440–3450.

Han, Y., He, M., Marin, T., Shen, H., Wang, W.T., Lee, T.Y., Hong, H.C., Jiang, Z.L., Garland Jr, T., Shyy, J.Y., Gongol, B., Chien, S., 2021. Roles of KLF4 and AMPK in the inhibition of glycolysis by pulsatile shear stress in endothelial cells. Proc. Natl. Acad. Sci. Usa. 118 (21), e2103982118 https://doi.org/10.1073/pnas.2103982118.

Hawkins, L.J., Al-Attar, R., Storey, K.B., 2018. Transcriptional regulation of metabolism in disease: From transcription factors to epigenetics. PeerJ 6, e5062. https://doi.org/10.7717/peerj.5062.

Kelly, B., O'Neill, L.A., 2015. Metabolic reprogramming in macrophages and dendritic cells in innate immunity. Cell Res. 25 (7), 771–784. https://doi.org/10.1038/cr.2015.68.

Kim, H.C., Mofarrahi, M., Vassilakopoulos, T., Maltais, F., Sigala, I., Debigare, R., Bellenis, I., Hussain, S.N., 2010. Expression and functional significance of nicotinamide N-methyl transferase in skeletal muscles of patients with chronic obstructive pulmonary disease. Am. J. Respir. Crit. Care Med. 181 (8), 797–805. https://doi.org/10.1164/rccm.200906-0936OC.

Laemmli, U.K., 1970. Cleavage of structural proteins during the assembly of the head of bacteriophage T4. Nature 227 (5259), 680–685. https://doi.org/10.1038/227680a0.

Li, J., You, S., Zhang, S., Hu, Q., Wang, F., Chi, X., Zhao, W., Xie, C., Zhang, C., Yu, Y., Liu, J., Zhao, Y., Liu, P., Zhang, Y., Wei, X., Li, Q., Wang, X., Yin, Z., 2019. Elevated N-methyltransferase expression induced by hepatic stellate cells contributes to the metastasis of hepatocellular carcinoma via regulation of the CD44v3 isoform. Mol. Oncol. 13 (9), 1993–2009. https://doi.org/10.1002/1878-0261.12544.

Li, Y.Y., Zhang, G.X., He, J.P., Zhang, D.D., Kong, X.X., Yuan, H.M., Chen, F.L., 2017. Ufm1 inhibits LPS-induced endothelial cell inflammatory responses through the NF-κB signaling pathway. Int. J. Mol. Med 39 (5), 1119–1126. https://doi.org/10.3892/ijmm.2017.2947.

Liu, L., Su, X., Quinn 3rd, W.J., Hui, S., Krukenberg, K., Frederick, D.W., Redpath, P., Zhan, L., Chellappa, K., White, E., Migaud, M., Mitchison, T.J., Baur, J.A., Rabinowitz, J.D., 2018. Quantitative Analysis of NAD Synthesis-Breakdown Fluxes. e5 Cell. Metab. 27 (5), 1067–1080. https://doi.org/10.1016/j.cmet.2018.03.018.

Mateuszuk, Ł., Khomich, T.I., Słomińska, E., Gajda, M., Wójcik, L., Łomnicka, M., Gwóźdź, P., Chłopicki, S., 2009. Activation of nicotinamide N-methyltrasferase and increased formation of 1-methylnicotinamide (MNA) in atherosclerosis. Pharmacol. Rep. 61 (1), 76–85. https://doi.org/10.1016/s1734-1140(09)70009-x.

Mateuszuk, Ł., Campagna, R., Kutryb-Zając, B., Kuś, K., Słomińska, E.M., Smolenski, R.T., Chłopicki, S., 2020. Reversal of endothelial dysfunction by nicotinamide mononucleotide via extracellular conversion to nicotinamide riboside. Biochem. Pharm. 178, 114019–114030. https://doi.org/10.1016/j.bcp.2020.114019.

Meng, F., Lowell, C.A., 1997. Lipopolysaccharide (LPS)-induced macrophage activation and signal transduction in the absence of Src-family kinases Hck, Fgr, and Lyn. J. Exp. Med 185 (9), 1661–1670. https://doi.org/10.1084/jem.185.9.1661.

Mistry, R.J., Klamt, F., Ramsden, D.B., Parsons, R.B., 2020. Nicotinamide N-methyltransferase expression in SH-SY5Y human neuroblastoma cells decreases oxidative stress. J. Biochem. Mol. Toxicol. 34 (3), e22439 https://doi.org/10.1002/jbt.22439.

Nejabati, H.R., Mihanfar, A., Pezeshkian, M., Fattahi, A., Latifi, Z., Safaie, N., Valiloo, M., Jodati, A.R., Nouri, M., 2018. N1-methylnicotinamide (MNAM) as a guardian of cardiovascular system. J. Cell. Physiol. 233 (10), 6386–6394. https://doi.org/10.1002/jcp.26636.

Onopiuk, M., Brutkowski, W., Young, C., Krasowska, E., Róg, J., Ritso, M., Wojciechowska, S., Arkle, S., Zabłocki, K., Górecki, D.C., 2015. Store-operated calcium entry contributes to abnormal Ca2+ signaling in dystrophic mdx mouse myoblasts. Arch. Biochem. Biophys. 569, 1–9.

Palsson-McDermott, E.M., Curtis, A.M., Goel, G., Lauterbach, M.A., Sheedy, F.J., Gleeson, L.E., van den Bosch, M.W., Quinn, S.R., Domingo-Fernandez, R., Johnston, D.G., Jiang, J.K., Israelsen, W.J., Keane, J., Thomas, C., Clish, C., Vander

Heiden, M., Xavier, R.J., O'Neill, L.A., 2015. Pyruvate kinase M2 regulates Hif-1α activity and IL-1β induction and is a critical determinant of the warburg effect in LPS-activated macrophages. Cell. Metab. 21 (1), 65–80. https://doi.org/10.1016/j.cmet.2014.12.005.

Przyborowski, K., Wojewoda, M., Sitek, B., Zakrzewska, A., Kij, A., Wandzel, K., Zoladz, J.A., Chlopicki, S., 2015. Effects of 1-Methylnicotinamide (MNA) on Exercise Capacity and Endothelial Response in Diabetic Mice. PLoS One 10 (6), e0130908. https://doi.org/10.1371/journal.pone.0130908.

Qiu, X., Liang, X., Li, H., Sun, R., 2021. LPS-induced vein endothelial cell injury and acute lung injury have Btk and Orai 1 to regulate SOC-mediated calcium influx. Int. Immunopharmacol. 90, 107039 https://doi.org/10.1016/j.intimp.2020.107039.

Robb, J.L., Hammad, N.A., Weightman Potter, P.G., Chilton, J.K., Beall, C., Ellacott, K.L. J., 2020. The metabolic response to inflammation in astrocytes is regulated by nuclear factor-kappa B signaling. Glia 68 (11), 2246–2263. https://doi.org/10.1002/glia.23835.

Roberti, A., Fernández, A.F., Fraga, M.F., 2021. Nicotinamide N-methyltransferase: At the crossroads between cellular metabolism and epigenetic regulation. Mol. Metab. 45, 101165 https://doi.org/10.1016/j.molmet.2021.101165.

Roessler, M., Rollinger, W., Palme, S., Hagmann, M.L., Berndt, P., Engel, A.M., Schneidinger, B., Pfeffer, M., Andres, H., Karl, J., Bodenmüller, H., Rüschoff, J., Henkel, T., Rohr, G., Rossol, S., Rösch, W., Langen, H., Zolg, W., Tacke, M., 2005. Identification of nicotinamide N-methyltransferase as a novel serum tumor marker for colorectal cancer. Clin. Cancer Res 11 (18), 6550–6557. https://doi.org/10.1158/1078-0432.CCR-05-0983.

Schlegel, N., Baumer, Y., Drenckhahn, D., Waschke, J., 2009. Lipopolysaccharide-induced endothelial barrier breakdown is cyclic adenosine monophosphate dependent in vivo and in vitro. Crit. Care Med 37 (5), 1735–1743. https://doi.org/10.1097/CCM.0b013e31819deb6a.

Sperber, H., Mathieu, J., Wang, Y., Ferreccio, A., Hesson, J., Xu, Z., Fischer, K.A., Devi, A., Detraux, D., Gu, H., Battle, S.L., Showalter, M., Valensisi, C., Bielas, J.H., Ericson, N.G., Margaretha, L., Robitaille, A.,M., Margineantu, D., Fiehn, O., Hockenbery, D., Blau, C.A., Raftery, D., Margolin, A.A., Hawkins, R.D., Moon, R.T., Ware, C.B., Ruohola-Baker, H., 2015. The metabolome regulates the epigenetic landscape during naive-to-primed human embryonic stem cell transition. Nat. Cell. Biol. 17 (12), 1523–1535. https://doi.org/10.1038/ncb3264.

Sternak, M., Khomich, T.I., Jakubowski, A., Szafarz, M., Szczepański, W., Białas, M., Stojak, M., Szymura-Oleksiak, J., Chłopicki, S., 2010. Nicotinamide N-methyltransferase (NNMT) and 1-methylnicotinamide (MNA) in experimental hepatitis induced by concanavalin A in the mouse. Pharmacol. Rep. 62 (3), 483–493. https://doi.org/10.1016/s1734-1140(10)70304-2.

Szewczyk, A., Jarmuszkiewicz, W., Kozieł, A., Sobieraj, I., Łukasiak, A., Skup, A., Bednarczyk, P., Drabarek, B., Dymkowska, D., Wrzosek, A., Zabłocki, K., 2015. Mitochondrial mechanisms of endothelial dysfunction. Pharmacol. Rep. 67, 704–710. https://doi.org/10.1016/j.pharep.2015.04.009.

Tomida, M., Ohtake, H., Yokota, T., Kobayashi, Y., Kurosumi, M., 2008. Stat3 up-regulates expression of nicotinamide N-methyltransferase in human cancer cells. J. Cancer Res. Clin. Oncol. 134 (5), 551–559. https://doi.org/10.1007/s00432-007-0318-6.

Ulanovskaya, O.A., Zuhl, A.M., Cravatt, B.F., 2013. NNMT promotes epigenetic remodeling in cancer by creating a metabolic methylation sink. Nat. Chem. Biol. 9 (5), 300–306. https://doi.org/10.1038/nchembio.1204.

Vijayan, V., Pradhan, P., Braud, L., Fuchs, H.R., Gueler, F., Motterlini, R., Foresti, R., Immenschuh, S., 2019. Human and murine macrophages exhibit differential metabolic responses to lipopolysaccharide - A divergent role for glycolysis. Redox Biol. 22, 101147 https://doi.org/10.1016/j.redox.2019.101147.

Wang, Y., Zeng, J., Wu, W., Xie, S., Yu, H., Li, G., Zhu, T., Li, F., Lu, J., Wang, G.Y., Xie, X., Zhang, J., 2019. Nicotinamide N-methyltransferase enhances chemoresistance in breast cancer through SIRT1 protein stabilization. Breast Cancer Res 21 (1), 64. https://doi.org/10.1186/s13058-019-1150-z.

Yang, J., Tong, Q., Zhang, Y., Yuan, S., Gao, Y., Deng, K., Wang, Y., Lu, J., Xie, X., Zhang, Z., Zhang, J., 2021. Overexpression of Nicotinamide N-methyltransferase mainly covers stroma of colorectal cancer and correlates with unfavorable survival by its product 1-MNA. J. Cancer 12 (20), 6170–6181. https://doi.org/10.7150/jca.56419.

Yarbro, J.R., Pence, B.D., 2019. Classical monocytes from older adults maintain capacity for metabolic compensation during glucose deprivation and lipopolysaccharide stimulation. Mech. Ageing Dev. 183, 111146 https://doi.org/10.1016/j.mad.2019.111146.

Yoshino, J., Imai, S., 2013. Accurate measurement of nicotinamide adenine dinucleotide (NAD⁺) with high-performance liquid chromatography. Methods Mol. Biol. 1077, 203–215. https://doi.org/10.1007/978-1-62703-637-5_14.

You, L., Zhang, D., Geng, H., Sun, F., Lei, M., 2021. Salidroside protects endothelial cells against LPS-induced inflammatory injury by inhibiting NLRP3 and enhancing autophagy. BMC Complement Med. Ther. 21 (1), 146. https://doi.org/10.1186/s12906-021-03307-0.